Appl Nanosci (2015) 5:521–525
DOI 10.1007/s13204-014-0345-y

ORIGINAL ARTICLE

The structure, morphology, and the metal-enhanced fluorescence of nano-Ag/ZnO core–shell structure

Yue Zhao · Yanli Ding · Xiang Peng · Mingtao Zhou · Xiaoyan Liang · Jiahua Min · Linjun Wang · Weimin Shi

Received: 14 March 2013 / Accepted: 29 July 2014 / Published online: 12 September 2014

Abstract Nano-polycrystalline silver (Ag) particles with the diameter of 60 nm were synthesized by the reducing agent sodium citrate. An amorphous zinc oxide (ZnO) shell layer was then coated on the surface of silver particles using wet chemical method. The Ag/ZnO core–shell structure was characterized by scanning electron microscope, transmission electron microscopy, ultraviolet–visible spectroscopy and fluorescence (FL) measurement. The results showed that nano-Ag/ZnO core–shell particles with an average diameter of ~100 nm were prepared successfully, and the FL intensity of Rhodamine 6G (R6G) mixed with Ag/ZnO nanoparticle was 53 % greater than that of the same amount of R6G without any nanoparticles, which may be related to the effect of surface plasmon resonance.

Keywords Silver particles · Ag/ZnO core–shell structure · Metal-enhanced fluorescence

Introduction

Fluorescence (FL) detection is a central technology in biological research and clinical chemistry. Engineering of advanced substrates is an effective way to improve the FL detection capability and to reduce the cost (Aslan et al. 2008). However, because the sensitivity of FL is still insufficient to meet the needs of some special fields, it is necessary to develop new methods to further enhance the sensitivity of FL detection. Some scientists found that the FL emission of dyes mixed with nano-metal particles could be strongly enhanced (Geddes and Lakowicz 2002), which was caused by surface plasmon resonance between metal nanoparticle and incident light (Aslan 2005). Many nanomaterials, such as gold, copper, silver and zinc, exhibit metal-enhanced fluorescence (MEF) (Ahamed et al. 2008). Comparing with other metals, silver has received much attention due to its excellent MEF properties (Chowdhury et al. 2006). However, the direct contact between metal particles and dyes might result in FL quenching due to the non-radiation energy transfer (Campion et al. 1980), therefore the spacer layer between metal particles and dye is necessary to eliminate this quenching effect.

ZnO is one of the most attractive oxide semiconductors used in MEF application. The MEF mechanism of ZnO nanostructure is due to the change in photonic mode density and/or reduction in self-quenching of fluorophores (Dorfman et al. 2006; Zhang et al. 2010; Yan-Song et al. 2012). In nanoparticles with core–shell structure, such as Au/ZnO (Krishna Kanta Haldar 2008), Ag/SiO_2 and ZnO/Ag (Li et al. 2010), new excited properties are found while the respective optical-electrical properties of the core and shell remain. In addition, the core–shell structure could be prepared by a number of methods, such as template-confined synthesis routes, high-temperature methods, hydrothermal synthesis (Li et al. 2008) and wet chemical methods (Xue-lin Tian et al. 2006).

In this report, the Ag particles were successfully prepared by chemical reduction and then the ZnO shell layer was coated onto the surface of silver particles using wet chemical method. The structure and the optical properties of the ZnO/Ag core–shell particles were studied by transmission electron microscopy (TEM), scanning electron

Y. Zhao (✉) · Y. Ding · X. Peng · M. Zhou · X. Liang · J. Min · L. Wang · W. Shi
Department of Electronic Information Materials, Shanghai Leading Academic Disciplines, Shanghai University, 200072 Shanghai, People's Republic of China
e-mail: zhaoyue1976@sohu.com

microscopy (SEM), ultraviolet–visible spectroscopy (UV–VIS) and FL.

Experimental

$AgNO_3$ (15.7 mg) was dissolved into 100 ml of de-ionized (DI) water in a beaker with magnetic stirring. The reducing agent, 1 % $C_6H_5O_7Na_3{\cdot}2H_2O$ (2 ml) was added into the $AgNO_3$ solution. Then, this mixed solution was magnetic stirring in an 80 °C water bath for 15 min. After reaction, the Ag-sol solution was removed and cooled to room temperature. Then, the Ag-sol was purified by centrifuging in ethanol three times.

The wet chemical method was used to coat the ZnO shell on Ag nanoparticles. The Zn $(NO_3){\cdot}6H_2O$ (14.9 mg) was dissolved in 10 ml DI water and then triethanolamine (NA) (1 ml) was added into this solution as an assistor. This as-prepared mixture was slowly poured into the as-prepared Ag-sol, followed by magnetic stirring in 80 °C water bath for about 2 h. Finally, the cooled Ag/ZnO sol was purified by centrifuging in ethanol three times.

The morphology of Ag/ZnO core–shell structure was observed using an SEM (JSM-6700F). In order to carry out the SEM observation, the SEM sample was prepared by the Ag/ZnO sol dripped on glass and then dried in air. A TEM (JEM-2010F) equipped with energy dispersive spectrometer (EDS) was used to observe the crystal structure and analyze the elemental distribution of Ag/ZnO core–shell structure. The Ag/ZnO–ethanol sol was dripped into copper mesh and then dried in air for TEM observation. FL measurements were carried out with a PL spectrometer (SPEX1403, SPEX) to study the optical properties using a 500-nm He–Cd laser as the excitation source. The optical absorbance spectra of as-prepared Ag nanoparticles and the Ag/ZnO core–shell structure were obtained by a UV–vis spectrophotometer (v-570, FASCO) in the visible ranges. The diameter of the Ag/ZnO core–shell nanoparticles was calculated by Image Tool (UTHSCSA) analysis of the SEM image and the TEM images. All measurements were carried out at room temperature under ambient atmosphere.

Results and discussion

The absorbance spectra of the AgNPs and the Ag/ZnO core–shell structure in DI water were presented in Fig. 1a, b, respectively. The absorption peak of the Ag nanoparticle was centered at 427 nm as shown in Fig. 1a. This peak corresponds to a transverse mode (TM) of the localized surface plasmon resonance (LSPR) of the nano-Ag

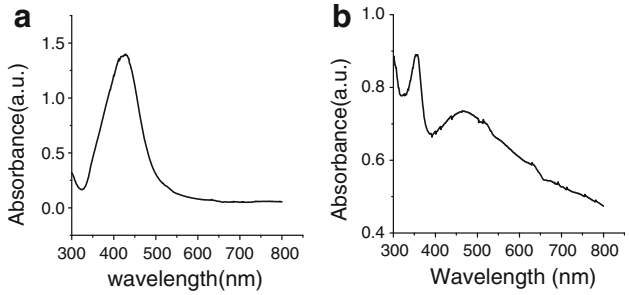

Fig. 1 UV–Vis spectra of the sliver particles (**a**) and the Ag/ZnO core–shell structure (**b**)

particles. According to Brus' theory (Brus 1986), the calculated particles size was about 60 nm. In addition, two absorption peaks centered at 467 and 356 nm are shown in Fig. 1b, which might be attributed to the absorption of the Ag nanoparticle and the ZnO shell layer, respectively. Comparing Fig. 1a and b, the absorption peak of the Ag nanoparticle was red-shifted from 427 to 467 nm. This observation was consistent with the results in the previous papers, in which the LSPR peaks of Ag nanoparticles coated with SiO_2 exhibited a significant red-shift. This phenomenon could be explained by the change of the refractive index surrounding the nano-Ag particles. The effect of the surrounding medium on the plasmon resonance wavelength of spherical nanoparticles could be qualitatively described as $\lambda_p = \lambda_{p,b}(2n_0^2+1)^{1/2} \approx 3^{1/2}\lambda_{p,b}\{1+\frac{1}{3}[n_0-1]\}$, where $\lambda_p$is the particle plasmon wavelength, $\lambda_{p,b}$ is the bulk plasmon wavelength, and n_0 is the index of refraction of the surrounding medium. Since coating a porous ZnO layer on the Ag nanoparticle, the surrounding medium could be considered as a compound of ZnO and air (Kelly et al. 2003). According to the effect medium theory (Choy 1999), the Maxwell–Garnett formula, the effect medium of this composite layer, ε_{eff}, could be estimated from $\frac{\varepsilon_{eff}-\varepsilon_{air}}{\varepsilon_{eff}-2\varepsilon_{air}} = f\frac{\varepsilon_{ZnO}-1}{\varepsilon_{ZnO}+2}$, where $\varepsilon_{air} \approx 1$ is the dielectric constant of air, ε_{ZnO} is the dielectric constant of ZnO, and f is the volume fraction of ZnO which increased with the continuous ZnO coating. The increasing f resulted in an increasing ε_{eff} , which demonstrated an increasingn_0. As a result, the LSPR peak of Ag nanoparticles was red-shifted continuously with the increasing n_0. Moreover, the theory absorption peak of nano-ZnO was centered at 370 nm, corresponding to the band gap of 3.46 eV (Zhu-xi et al. 2002). But in this paper, the LSPR peak of nano-ZnO shell was blue shifted from 370 to 356 nm, which might be caused by the quantum size effect (Asl et al. 2011). As shown the HRTEM image in Fig. 3b, the amorphous ZnO shell layer existed on the surface of Ag particle, and some small ZnO nano-crystals might be included in this shell layer, which could lead to the blue-shift of the LSPR peak of nano-ZnO layer.

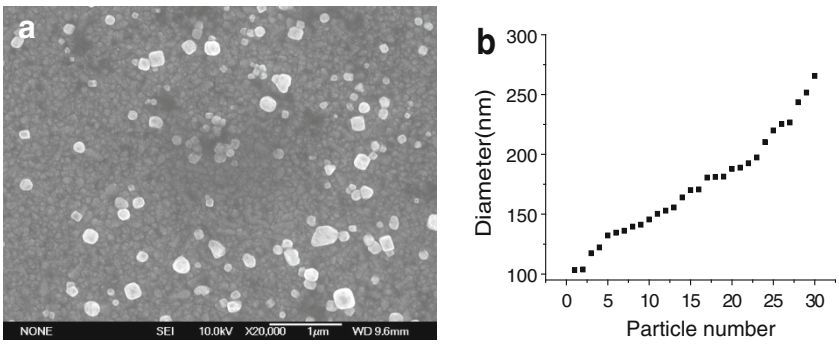

Fig. 2 The SEM image of Ag/ZnO core–shell particles (**a**) and the diameter distribution of the particles in SEM image (**b**)

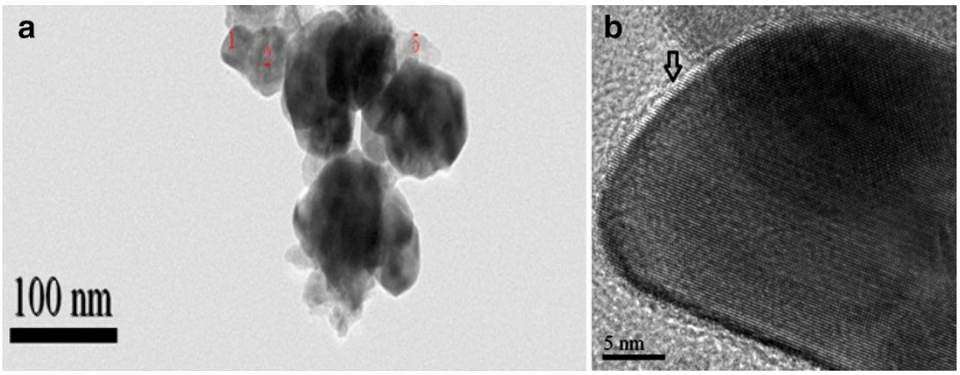

Fig. 3 TEM images of the Ag/ZnO composite structure (**a**) and the HRTEM image of the selected area (1) in TEM image (**b**)

Figure 2a shows the SEM image of the surface morphology of Ag/ZnO core–shell particles on the FTO glass. It was observed that the nanoparticles were dispersed in the glass substrate and the shape of composite particles was irregular. Figure 2b shows the diameter distribution of the particles in Fig. 2a. The diameter of the particles was in the range of 100–260 nm and the average diameter of these particles was about 188 nm. However, the diameter of several particles was over 260 nm or below 100 nm. A large range of the diameter of the Ag/ZnO core–shell particles in SEM image might be attributed to the agglomeration of nanoparticles, which was caused by the bond energy (van der Waals forces), the magnetic forces or the surface purity in the surface of the Ag/ZnO core–shell particles (Shen et al. 2009).

The TEM image is shown in Fig. 3a, which gave the structural morphology of the Ag/ZnO core–shell particles. The darker part in image was considered to be the Ag core particles and the light color place is the ZnO shell layer, which could be confirmed by the EDS results in Fig. 4. Figure 3b is the HRTEM image of the select area (1) in Fig. 3a. Furthermore, the boundary of the Ag core and the ZnO shell layer is shown by the black arrow in Fig. 3b. It is clearly seen that the Ag particle was coated by a thin ZnO shell and the lattice parameter of Ag nanoparticle was about 0.230 nm, which corresponds to the (111) planes (Qiu et al. 2007). The image in Fig. 3 also gave evidence that the ZnO shell was an amorphous structure and its calculated thickness was about 20–40 nm. Moreover, the calculated average diameter of the Ag core was about 60 nm, but this conclusion was not consistent with the result in Fig. 2a, which was due to the aggregates of Ag/ZnO core–shell structure in SEM samples, as discussed above.

The element distribution of Ag/ZnO core–shell particles was obtained by EDS measurement, as showed in Fig. 4. Figure 4a shows the element distribution of the select location (1) in Fig. 3a, and Fig. 4b shows that of the select location (2) in Fig. 3a. Both Fig. 4a, b shows that the select location (1) or (2) was consisted of the vast majority of silver and only a small part of the zinc oxide. Figure 4c shows the element distribution of the select location (5) in Fig. 3a and the dominant nano-ZnO was existed in this select location. The element Cu might come from the copper mesh and no any other element could be found in the EDS results.

Figure 5 is the room temperature FL spectra of different solution. It shows that the FL emission peak of Rhodamine 6G (dye) was centered at 554 nm (Zhu et al. 2007), as shown in Fig. 5c. Curve (a) in Fig. 5 gives the FL emission of the sample prepared by the equal amount of dye mixed with Ag/ZnO particles. Furthermore, the FL peak of the sample prepared by the dye mixed with Ag particles was exhibited in the curve (b). In addition, no FL emission of the Ag/ZnO particles solution without dye was shown in Fig. 5d. The result clearly shows that both the Ag/ZnO and the Ag particles could enhance the FL emission intensity of the dye. The FL intensity of R6G mixed with Ag/ZnO

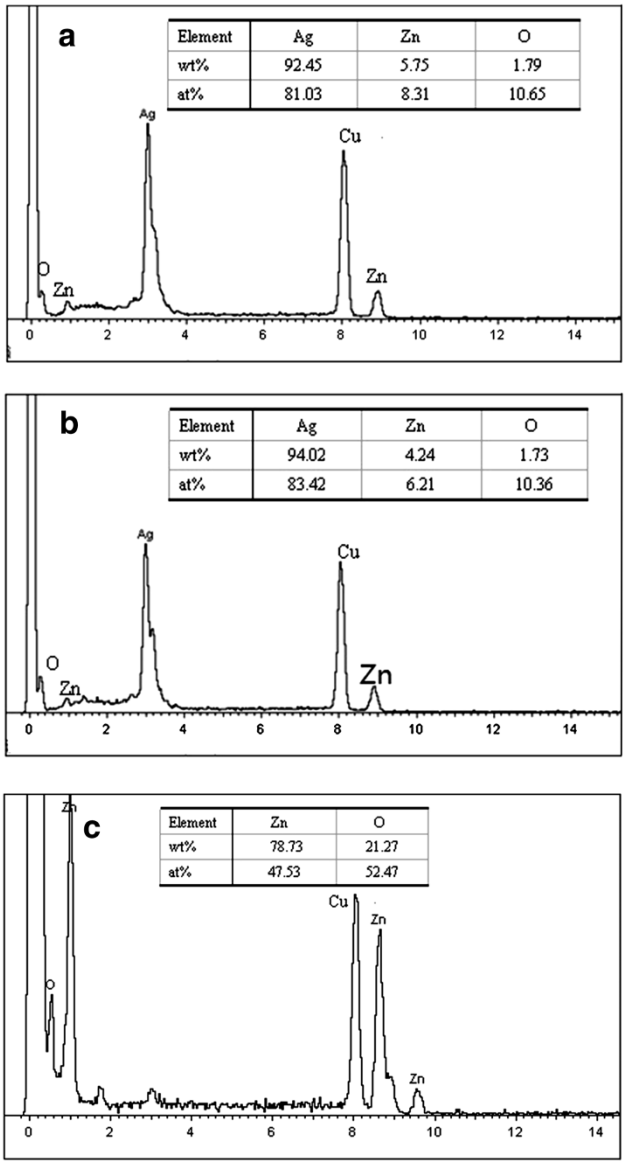

Fig. 4 EDS spectra of Ag/ZnO core–shell particles in TEM image, **a** selected area (1); **b** selected area (2); **c** selected area (5)

nanoparticle was 53 % larger than that of the same amount of R6G without any nanoparticles, which might be enhanced by the plasmonic interaction of metal surface. This result indicates that the ZnO shell was used to maintain a certain distance between the fluorescent molecule and the metal core, which caused the interaction between the surface plasmon and excitation light field to produce a FL emission enhancement. Furthermore, the ZnO shell layer also could enhance the FL emission of dye, which was caused by the change in photonic mode density and/or reduction in self-quenching of fluorophores for ZnO nanostructure (Satriano 2012). But the FL intensity of R6G mixed with Ag nanoparticle was only 13 % larger than that of the same amount of R6G solution, which might be due

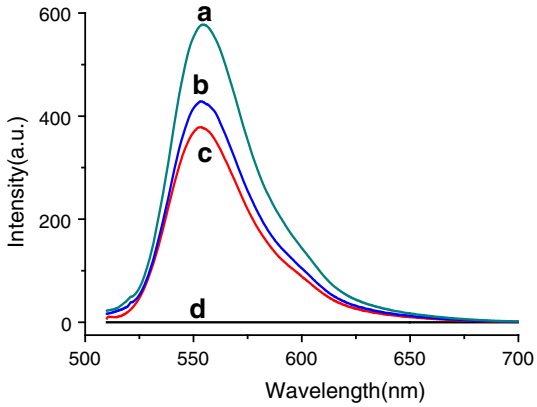

Fig. 5 Photoluminescence emission spectra of the dye mixed with Ag/ZnO particles (*a*), the dye mixed with Ag particles (*b*), R6G (*c*) and Ag/ZnO particle without dye (*d*)

to the non-radiation energy transfer between dye molecular and the metal (Yang et al. 2011).

Conclusion

In summary, the Ag/ZnO core–shell structure was successfully prepared through a simple and reliable method, which is less reported in the publications. The average diameter of nano-Ag/ZnO core–shell particles was about 188 nm. The FL intensity of R6G mixed with Ag/ZnO nanoparticle was 53 % larger than that of the same amount of R6G without any nanoparticles. But the FL intensity of R6G mixed with Ag nanoparticle was only 13 % larger than that of the same amount of R6G solution. Moreover, the preparation process of Ag/ZnO core–shell structure might be further improved in future experiments and post-treatment must be used to promote the crystallization of the ZnO shell layer. In addition, this optimized Ag/ZnO core–shell structure might be used for FL bio-sensing applications in future.

Acknowledgments This work was supported by Program for Changjiang Scholars, Innovative Research Team in University (No: IRT0739), Shanghai Leading Academic Disciplines (S30107), the National Natural Science Foundation of China (No. 60906043; No. 51102162) and Shanghai Natural Science Foundation (09ZR1409200).

References

Ahamed M, Karns M, Goodson M, Rowe J, Hussain SM, Schlager JJ, Hong Y (2008) Toxicol Appl Pharmacol 233:404–410

Asl SK, Rad MK, Sadrnezhaad SK (2011) AIP Conf Proc 1400:425–428
Aslan K, Lakowicz JR, Geddes CD (2005) Curr Opin Chem Biol 9:538–544
Aslan K, Previte MJ, Zhang Y, Gallagher T, Baillie L, Geddes CD (2008) Anal Chem 80(11):4125–4132
Brus L (1986) J Phys Chem 90:2555–2560
Campion A, Gallo AR, Harris CB, Robota HJ, Whitmore PM (1980) Chem Phys Lett 73:447
Chowdhury MH, Aslan K, Malyn SN, Lakowicz JR, Geddes CD (2006) Appl Phys Lett 88(17):173104
Choy TC (1999) International series of monographs on physics 1999. Clarendon Press/Oxford University Press, Oxford/New York
Dorfman A, Kumar N, Hahm JI (2006) Langmuir 22:4890–4895
Geddes CD, Lakowicz JR (2002) J Fluoresc 12(2):121–129
Kelly KL, Coronado E, Zhao LL, Schatz GC (2003) J Phys Chem B 107(3):668–677
Haldar KK, Sen T, Patra A (2008) J Phys Chem 112:11650–11656
Li C, Liu X, Yang P, Zhang C, Lian H, Lin J (2008) J Phys Chem 112:2904–2910
Li F, Wua J, Qin Q, Li Z, Huang X (2010) Superlattices Microstruct 47:232–240
Qiu X, Li L, Tang C, Li G (2007) J Am Chem Soc 129:11908–11909
Satriano C, Fragala ME, Aleeva Y (2012) J Colloid Interface Sci 365:90–96
Shen XS, Wang GZ, Hong X, Zhu W (2009) Phys Chem Chem Phys 11:7450–7454
Tian XL, Wang WH, Chen K, Cao GY (2006) Chin J Chem Phys 19(4):362–366
Yang J, Zhang F, Chen Y, Qian S, Hu P, Li W, Deng Y, Fang Y, Han L, Luqman M, Zhao D (2011) Chem Commun 47:11618–11620
Yan-Song L, Y Fu, Badugu R, Lakowicz JR, Xiao-Liang X (2012) Chin Phys B 21(3):037803
Zhang J, Thurber A, Tenne DA, Rasmussen JW, Wingett D, Hanna C, Punnoose A (2010) Adv Funct Mater 20(24):4358–4363
Zhu G, Gavrilenko VI, Noginov MA (2007) J Chem Phys 127:104503
Zhu-xi F, Bi-xia L, Yi-ping H, Gui-hong L (2002) Chin J Lumin 23(6):559–562